2

SOLID EARTH MODELLING PROGRAMME

Global Positioning System (GPS) based Geodesy had become capable of yielding sub-cm precision in location by the early 1990s and the possibility of it being used to determine crustal strain rates in India was recognised at C-MMACS in 1993 following the Khillari earthquake. Research at C-MMACS has since yielded fairly well constrained figures for the velocity of the Indian plate and the partitioning of strain from Kanya-Kumari to Ladakh in the trans-Himalyas. Over the years C-MMACS has also taken up the arduous task of setting up GPS stations in remote locations in the country to generate the required data base, and to extend application of GPS technology to other areas.

Inside

2.1 Interseismic Deformation Rates in Garhwal and Ladakh Himalaya

Global Positionaing System (GPS) campaign data collected in the Garhwal Himalayas in 2005 (Figure 2.1) has been analysed along with the earlier GPS campaign data set (1995 to 2004) of the Garhwal Himalayas available at C-MMACS to give regional deformation over a period of 10 years in the Garhwal Himalayas. The results from the above analysis indicate a significant regional deformation of 10mm/yr between the Garhwal GPS campaign stations in the Main Central Thrust (MCT) zone. Hence it is essential to establish a very dense network of campaign stations in the MCT zone starting from the Chamoli-Joshimath area in the east to the Uttarkashi-Bhatwari area in the west and to make GPS measurements every six months in this region.GPS campaign data collected in Ladakh Himalayas (Figure 2.2) in 2006 and 2008 has been analysed along with the earlier GPS campaign data set (1997 to 2002) of the Ladakh Himalayas to give the regional deformation in this region and also a well constrained slip rate of the Karakoram fault. Priliminary results of campaign GPS data from Ladakh indicate that there is no significant internal deformation within Ladakh, and that all move at 30 to 32 mm/yr north east, in the ITRF 2000 reference frame.

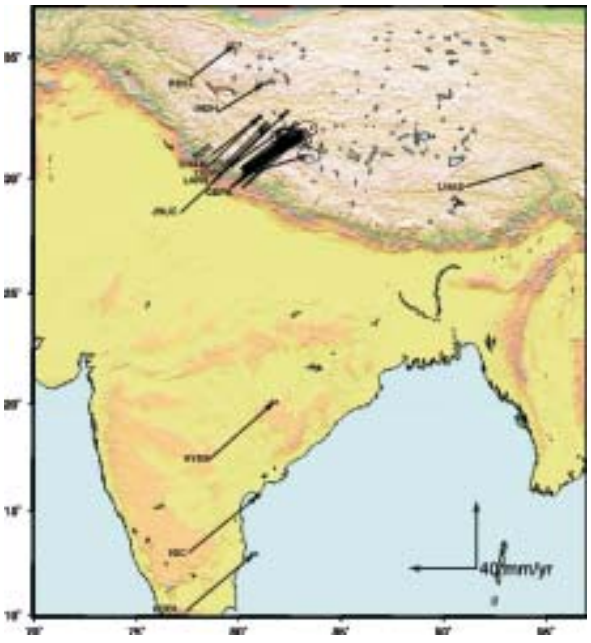

Figure 2.1 ITRF 2000 Velocities of Gharwal Himalaya sites (1995-2005)

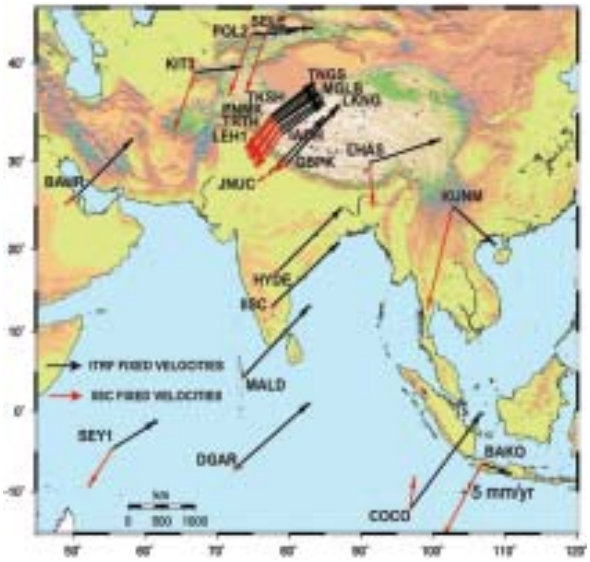

Figure 2.2 GPS derived velocities of Ladakh Himalaya sites in ITRF 00 (1997-2008)

Sridevi Jade, M S M Vijayan, M B Ananda and P Dileep Kumar

2.2 Regional Deformation Pattern in Darjeeling-Sikkim

Geodetic Global Positioning System measurements in the Darjiling-Sikkim Himalaya (DSH) indicate that the frontal part of the Darjiling Himalaya is locked to the Indian plate and statistically negligible shortening is accumulating there at present. The results also indicate that there is a fair amount of heterogeneity in the way convergence is accommodated along the length of the Himalayan arc and Himalayan seismic hazard estimations need to account for this.

Seismicity patterns in the DSH (Figure 2.3) indicate that active deformation in the area is driven by strike-slip as well as thrust tectonics. Strain accumulation in the DSH during 2000-2004 appears to be dominated by strike-slip

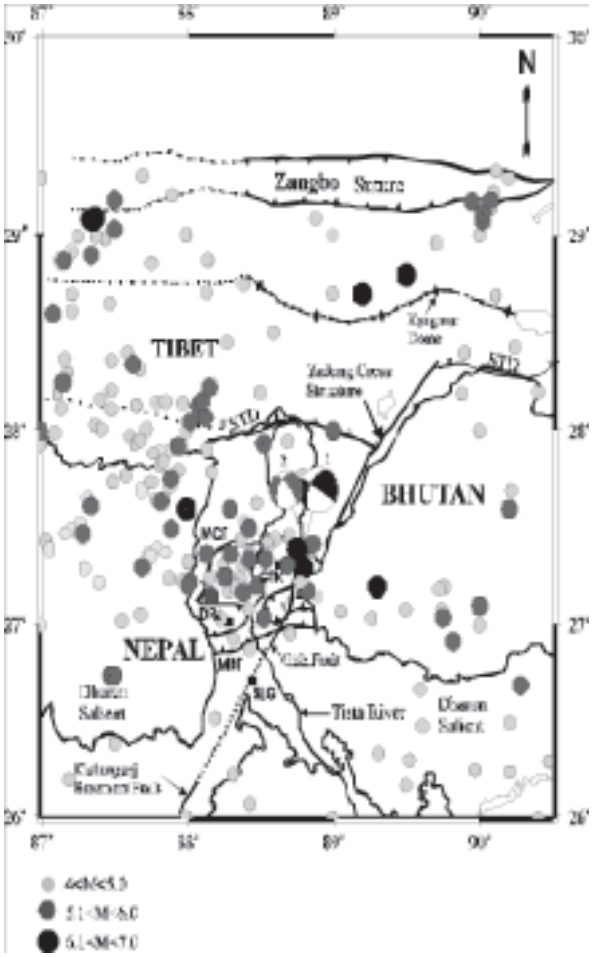

Figure 2.3 Map showing the main faults, distribution of earthquake foci between 1800 and 2006 (Sources: ISC, NOAA, IMD, NEIC) in the Darjiling-Sikkim and surrounding area

tectonics in the region and about ~ 4-5 mm/yr of sinistral strike-slip is observed along a NNE-SSW trending near-vertical Gish transverse fault.

Malay Mukul, Sridevi Jade and Abdul Matin

2.3 Quantification of Deformation Pattern in Indian Plate

The present-day Indian plate (Figure 2.4) is defined by the region between the Carlsberg Ridge in the Indian Ocean (the southern divergent plate boundary) and the Himalaya (northern convergent plate boundary). The eastern and western boundaries of the present-day Indian plate are more complex.The

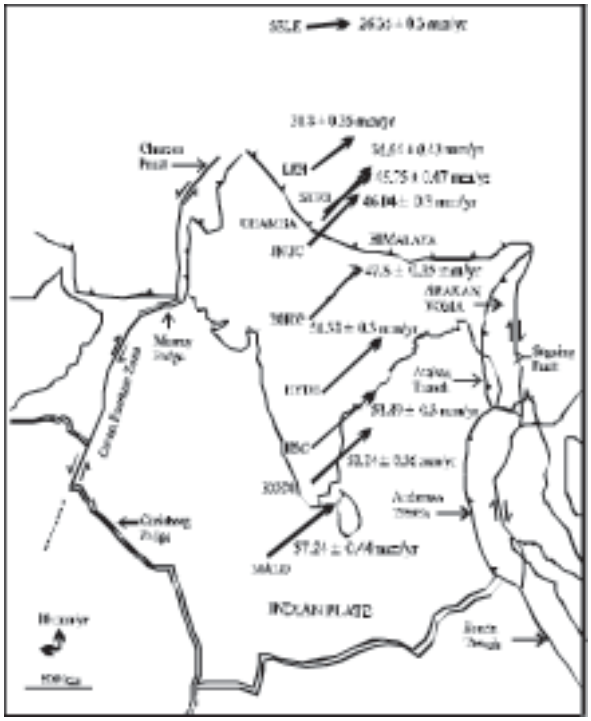

Figure 2.4 : Indian plate and plate boundaries with GPS velocities in ITRF 2000

western boundary is a composite boundary and is defined by the Owen fracture zone connecting the Carlsberg ridge with Murray Ridge and the dextral, transform, Chaman fault connecting the Murray ridge with the Himalaya .The eastern boundary is defined by the dextral Sagiang fault and the Sunda-Araken trench that extends into the Indo-Burman region as the Indo-Burman Fold Thrust Belt (IBFTB) in the Arakan Yomas. Given that the Indian plate motion occurs on the spherical earth, the motion is characterized by an Euler pole of rotation and an angular velocity corresponding to rotation about the pole. Several Euler poles of rotation have been computed by different authors using different sets of stations on the Indian plate in the ITRF 2000 reference frame. The composite Indian ITRF 2000 Euler pole computed using all the estimated Euler poles is determined as 51.33±1.79 N; 12.7±1.94 S. The composite angular velocity of the Indian plate in the ITRF 2000 reference frame is 0.479 ± 0.006 Myr-1. The nature of variation in the plate velocity within a given plate from one

boundary to the other is an important question because it determines the regions of strain accumulation in the plate. Plate velocities measured in the Indian plate (in the ITRF 2000 reference frame) from south to north (approximately along the 77-78E longitudes) vary from ~ 57 mm/year in the Maldives (04.19 N) to ~ 46 mm/yr in Delhi (28.54N) gradually. The Indian plate slows down by ~ 25 mm/yr from near its southern divergent boundary to its northern convergent boundary; the maximum deceleration of the Indian plate occurs north of 30 N latitude in the higher Himalayan region. This region is also likely to accommodate maximum strain because of this deceleration.

Sridevi Jade and Malay Mukul

2.4 Postseismic Deformation Modeling in the Andaman-Nicobar Region Following the Giant 2004 Sumatra-Andaman Earthquake

GPS measurements in the Andaman-Nicobar region (Figure 2.5), suggest intense postseismic deformation in the region following the 26 December 2004 Sumatra-Andaman earthquake whose 1400 km long rupture in the frontal arc of Sunda subduction zone extended from N Sumatra till north of North Andaman.

All the sites in the region experienced west to southwest motion during the postseismic period, which is similar to the observed coseismic displacement in the region. Postseismic uplift occurred at all sites, whereas the 2004 earthquake caused coseismic subsidence at most of the sites in the Andaman Nicobar region, except at those in the Little and North Andaman. Postseismic deformation follows a logarithmic decay with a decay time of about 70 days. In general, the postseismic horizontal deformation rate decreases from south to north. The horizontal and vertical deformation rates decrease from east to west which place strong constraints on the location of the afterslip in the Andaman region. Results indicate that in the Andaman region, the afterslip patch lies about 40 km east of the Andaman island belt, downdip of the coseismic rupture. In the Little Andaman and Nicobar region, the afterslip patch partly overlaps the coseismic rupture. The downdip edge of the afterslip patch on the subduction interface does not extend beyond the WAF (West Andaman fault) and SFS (Sumatra Fault System) in the Nicobar region.

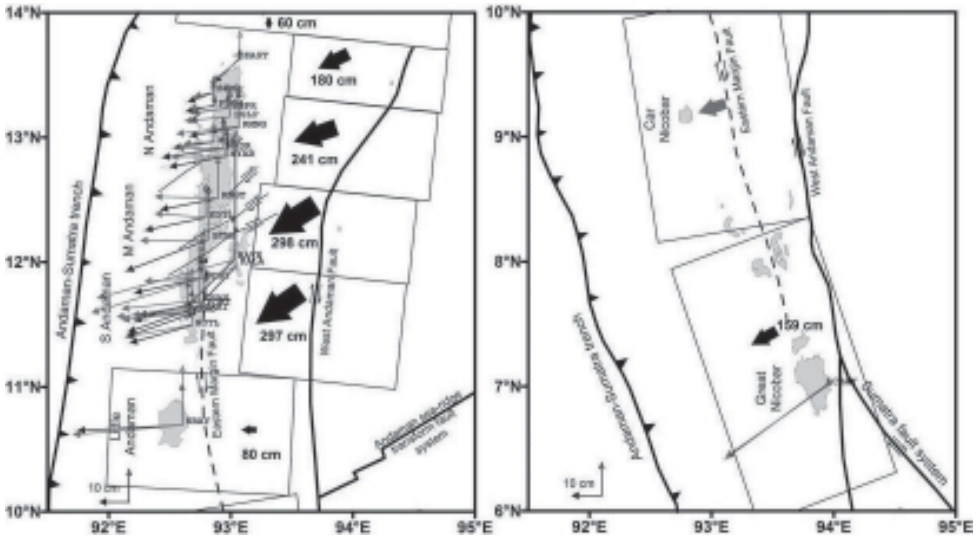

Figure 2.5 : Modelled (Bold Arrow) and Measured (Thin arrow) post seismic displacements in Andaman and Nicobar region. The rectangles denote surface projection of after slip patch

The aftershocks in the region contribute only 13% of the afterslip moment, implying that the afterslip in the region is mostly aseismic. The evolution of postseismic displacement and aftershocks appear to be having a linear relationship with different decay rates, consistent with the mechanism of frictional afterslip. The return period of grid earthquake having comparable slip is estimated to be above 400 years from the measured inter, 10+ post seismic rates.

V K Gahalaut, Sridevi Jade, J K Catherine, R Gireesh, M B Ananda, P Dileep Kumar, R Narsaiah, S S H Jafri, A Ambikapathy, A Bansal,R. K. Chadha, D C Gupta, B Nagarajan and S Kumar

2.5 GPS Based Precise Correction to the Arrival Time of Cerenkov Photons

The High Altitude GAmma Ray (HAGAR) telescope - an array of seven telescopes - has been established at the Indian Astronomical Observatory(IAO), Hanle to record Cerenkov photons created by gamma-rays in the atmosphere to nanosecond accuracy (Figure 2.6). The method of detection of front Cerenkov photons involves modelling the wave for which the arrival time correction to different telescopes is necessary. In turn, the arrival time correction and its accuracy depends on the accurate position of each telescopes. An experiment (Figure 2.7) has been designed to estimate the relative position of the telescopes with respect to the central pier and absolute position of each telescopes in the International Terrestrial Reference Frame (ITRF) 2005 to the required accuracy using geodetic dual frequency Global Positioning System (GPS) receivers. The designed experiment was conducted in May 2008 and the data was analysed along with International GNSS Service (IGS) stations data (Figure 2.7) using GAMIT/GLOBK software. The position estimates, with the maximum uncertainty of two millimetre, of each pier with respect to the centre pier was estimated. Estimated relative positions will in turn be used to calculate the difference in arrival time of the Cerenkov photons which is in the range of 1ms to 100ms. Accurate estimates of expected delay in arrival time of photons, derived from GPS positioning, due to the difference in position of each telescope with the central pier is vital in identifying the source of Cerenkov photons.

M S M Vijaya P Dileep Kumar, Tushar Prabhu, Sridevi Jade, Dorje Angchuk and Shrungeswar

Figure 2.6 HAGAR Telescopes at Indian Astronomical Observatory (IAO) Hanle

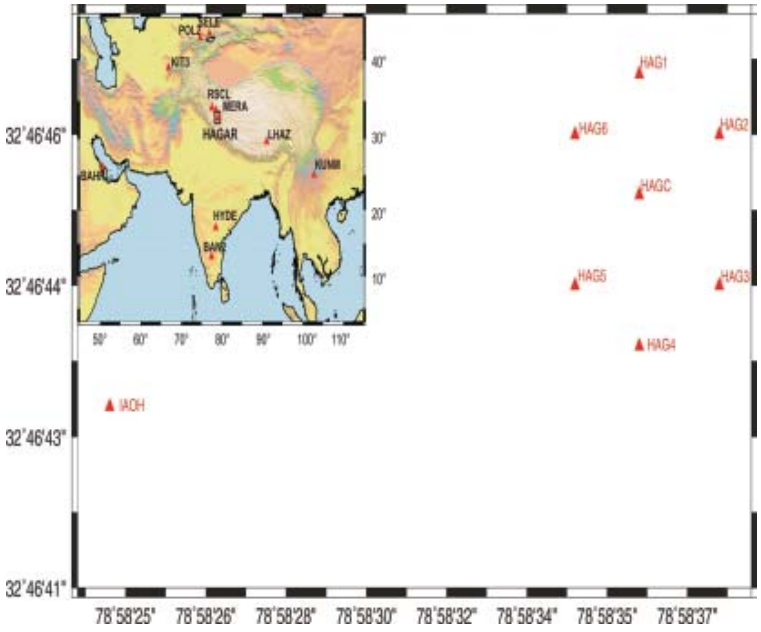

Figure 2.7 GPS stations used in the data analysis. Insert shows the IGS stations used in this anlaysis and the location of HAGAR in Indian regional map

2.6 GPS Derived Deformation Rates (1996-2008) in Andaman and Nicobar Islands

CMMACS has established GPS sites in Andaman and Nicobar Islands (Figure 2.8) in 1996 which have been reoccupied since then. During this period the Sumatra-Andaman mega earthquake of 2004 occurred displacing this region by meters. Analysis of GPS data of these sites for past 12 years has given inter-seismic, co-seismic and post-seismic deformation rates in this region. Horizontal inter-seismic (1996-2003) motion of this region in ITRF05 has been estimated to be as 29.7 mm/yr N, 33.3 mm/yr E and negligible vertical interseismic motion. Motion of Port Blair with respect to Indian Plate is estimated using Euler Pole for Indian Plate motion to be 9 mm/yr N 254° which represents elastic strain accumulation during the interseismic period. Co-seismic horizontal displacement due to the 2004 earthquake has been estimated as 1.6 (Havelock Island) to 6.6 m (Car Nicobar) in a predominantly WSW to southwest direction. Coseismic subsidence of 1-2 m occurred on

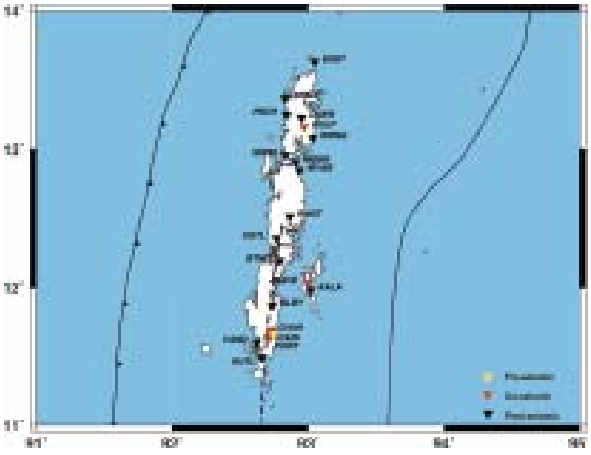

Figure 2.8 GPS sites in Andaman and Nicobar Islands (1996-2008)

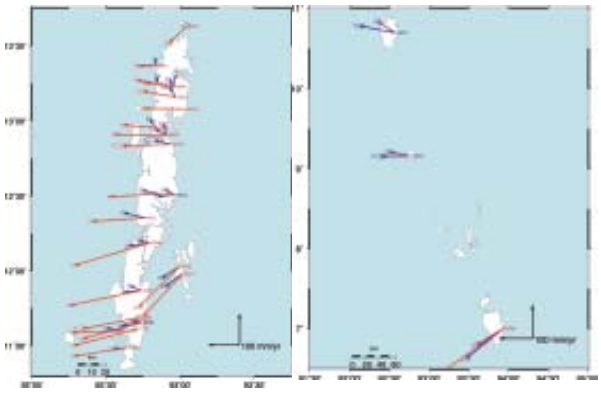

Figure 2.9 Post seismic deformation (2005-2008) in ITRF05

the east coast of the Andaman-Nicobar region, except in North and Little Andaman, where coseismic uplift of the order of 0.5-1.0m was reported. Post-Seismic displacement (2005-2008) from observation is estimated (Figure 2.9) to be 25 to 250 mm/yr with changing direction from SW (2005) to NE (2008) indicating the slow transition from post-seismic to inter-seismic motion. All the sites show post-seismic uplift ranging from 4 to 300 mm/yr.

Sridevi Jade, Anil Earnest, M S M Vijayan, M B Ananda, P Dileep Kumar

2.7 Reoccupation of Geodetic Bench-marks at Andaman and Nicobar Islands

To continuously monitor the post-seismic deformation due to the Andaman Nicobar Islands after the devastating December 26, 2004 megathrust earthquake, we have carried out precise geodetic surveys at most of the earlier established control points(Figure 2.10) at Andaman and Nicobar Islands during January-February 2009. These measurements will yield insight into the continuous post-seismic relaxation pattern in A&N Islands through the estimates of after slip and poro-elastic deformation. These simulations are extremely significant for future disaster mitigation aspects.

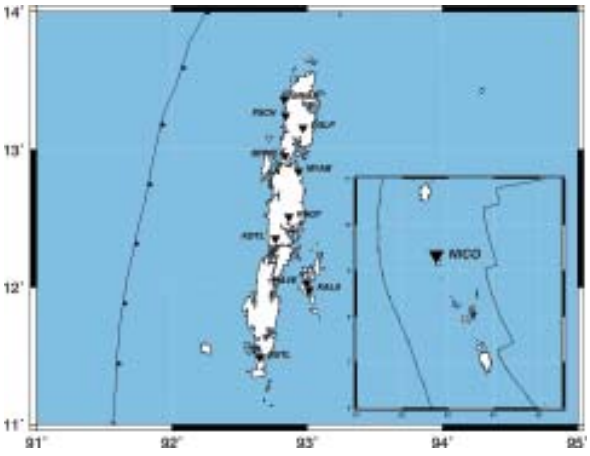

Figure 2.10: GPS sites monitored during January-February 2009

Anil Earnest, M S M Vijayan, and Sridevi Jade

2.8 Map of Seismic Hazard of India using Bayesian Approach

The problem of seismic hazard assessment has a lot of tools for its solution. Here the emphasis is given to purely statistical procedures and do not touch methods, which involve direct solution of wave propagation. The advantage of statistical approach is based on its generality. It does not need to identify values of different parameters, which we must know if we try to solve differential equations most of which could not be defined with sufficient accuracy. Among statistical methods the Bayesian approach is of special interest which comes from its ability to take into consideration uncertainty of parameters in fitted probabilistic laws and a priori given information. These properties of the Bayesian approach make it rather popular in seismic hazard investigations. Here, the Bayesian procedure is applied using the available seismic catalog of India with the purpose of estimating maximum seismic peak ground acceleration. The method is rather straightforward and needs only seismic catalog and attenuation law. At the same time it allows us to take into consideration the uncertainty of seismological information and thus possesses the main advantage of Bayesian approach.

The problem for maximum peak ground accelerations estimates essentially differs from those concerning maximal magnitudes. Finally, direct measurements of seismic accelerations are very rare and fragmental. That is why there are no catalogs, containing values of maximal accelerations for most interesting sites, but there are a lot of so called attenuation laws, which represent some functions between

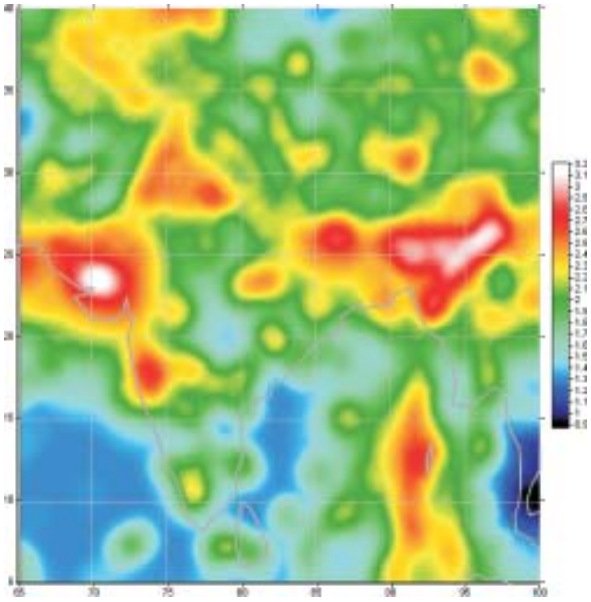

Figure 2.11 Map of maximum lg(A_{max}) in cm/sec^2, calculated according to attenuation law and catalogue

logarithm of maximal accelerations R = lg(A_{max}) and magnitude M of the earthquake and distance (km) from the considered site to epicenter of the earthquake:

$$R = \lg(A_{max}) = \psi(M,D) \qquad (1)$$

Usually function (1) is an empirical regression law, obtained by collecting data from a specified region and fitting to them some class of functions. In this study, the inputs used to estimate the seismic hazard are earthquake catalogue and seismic attenuation law i.e. the variation of peak ground acceleration of various magnitudes with hypocentral distances. The earthquake catalogue of the Indian subcontinent has been compiled from National Oceanic and Atmospheric Administration (NOAA), International Seismological Centre (ISC), National Earthquake Information Centre (NEIC) and several publications from Indian and international reputed journals.

The semi-empirical attenuation law of Parvez et al., (2001, 2002) has been used for calculation of A_{max}, which was defined for magnitudes $M \geq 5$. For small magnitudes, the following form has been used

$$\lg(A_{max}) = 0.54M - 1.5.\lg(D+10)+1.25, \; M < 5$$

which was derived for the whole world in [Steinberg et al., 1993].

Thus, after performing estimates in each node of the grid we have the plot of the following maps of maximum estimated values R_t, the map of estimates for maximum possible value of lg(A_{max}) the map of standard deviation for -estimates and the map of 90%-quintile of distribution of maximum values of apparent lg(A_{max}) on the future time interval of the length $T=100$ years. Figure 2.11 shows maximum lg(A_{max}) in cm/sec^2, calculated according to the attenuation law and catalog.

The proposed method in this study for estimating probabilistic characteristics of maximal values of seismic peak ground acceleration on a given future time interval for a given site is rather simple in use and needs only those information, which is in seismic catalogs and used attenuation laws.

Imtiyaz A Parvez and Alexey A Lyubushin

2.9 Microtremor Ambient Noise Experiment in Lower Reaches of Narmada valley, Western India

The lower reaches of Narmada valley has been investigated under the ongoing Department of Science and Technology initiation on "Studies of Shallow Science" given to University of Baroda. The work has inspired us to generate additional subsurface information (100m to 300m) applying H/V spectral ratio method, also called Nakamura technique, so as to understand the role of Quaternary floor over geomorphic features and resolve lithological breaks within the Quaternary sedimentary sequence.

A preliminary work was carried out using the 'Lennartz-LE-3D/5s' Seismometer & 'City

Shark II' Data acquisition system. These instruments are commonly used for site-specific seismic hazard (microzonation), however, in the present study; we have used them for decoding details regarding shallow Quaternary deposits. A grid based microtremor survey was adopted for preliminary studies, using one set of instruments, during the March 2009 field season. A single station noise recording method was adopted so as to extract geological information as suggested by Nakamura 1989; Lermo & Chavez Garcia, 1994. The microtremor data acquisition was carried out at two different resolutions. The low resolution seismic survey was carried out at a grid interval of 5km covering 470 sq. km area including the villages/towns like Govali-Ankleshwar- Bharuch Sukaltirth - Nareshwar, whereas high resolution microtremor survey was undertaken at 500m grid interval covering 7.3sq. km area around village Govali (Figure 2.12).

The Lennartz 5 sec seismometer and City

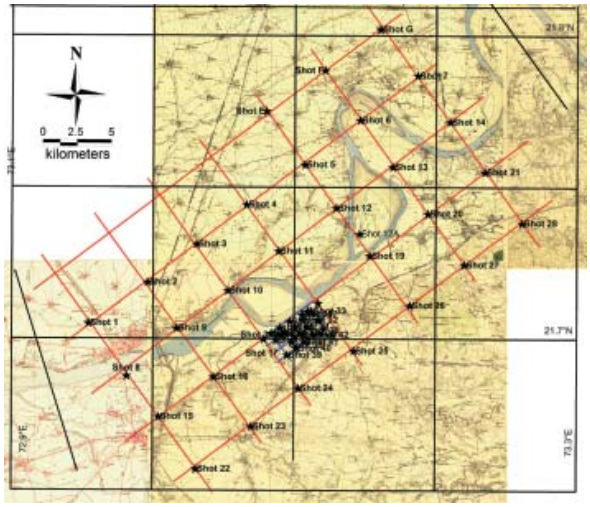

Figure 2.12 The sites used for the study at low resolution with an area of 470 sq km.

Shark II' Data acquisition system have been used to record three components of ambient noise at 60 different sites as shown in figures 1 and 2. Each station has recorded 30-40 minutes with a sample rate of 100 Hz. The response of the seismometer is flat to velocity between 0.2 and 50 Hz. Data analysis was focused in the frequency range between 0.2 and 20 Hz. In this work for each site the recording system operated continuously for 20 min with a sample rate of 100 Hz. Ambient noise data were processed in two stages. First, for each ambient noise recording, a number of windows, having duration of 20 sec each, were selected in order to exclude portions with unrealistically large amplitudes or spikes. The following steps were applied on the ambient noise data: (a) offset correction, (b) computation of Fourier spectra in all three components (E-W, N-S, Vertical), (c) application of a cosine taper, (d) smoothing of the Fourier amplitude spectra.

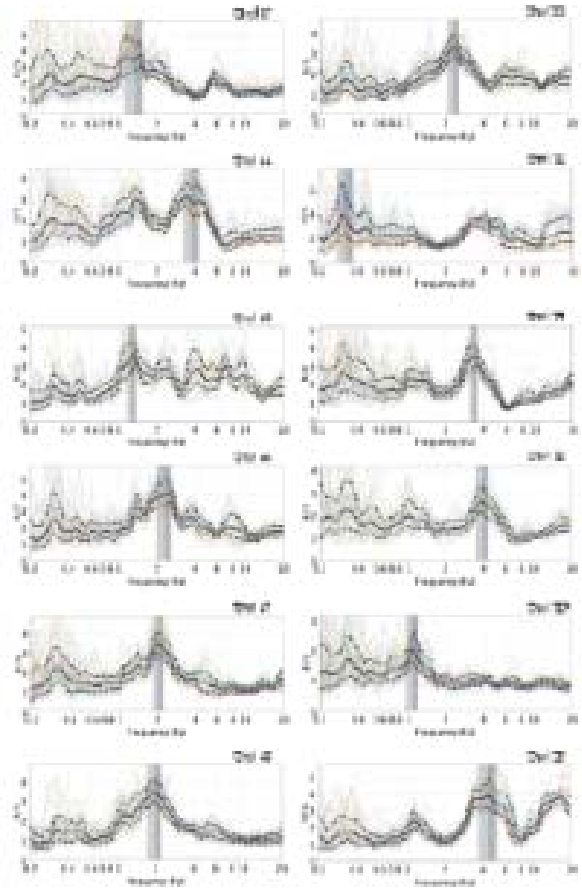

Figure2.13 Examples of H/V spectral ratio for different sites used in the study,

Figure 2.13 shows the H/V spectral ratio with fundamental frequency. The variation in the fundamental frequencies shows the variation in the thickness of the sedimentary basin in Narmada valley as it varies between 0.35-4.5 Hz.

The preliminary results are encouraging meeting both objectives to map the floor of the Quaternary sediment as well as identifying breaks at shallow depths using the empirical relation and Figure 2.14 shows one of the examples of converting the fundamental frequency into thickness of the sedimentary layer.

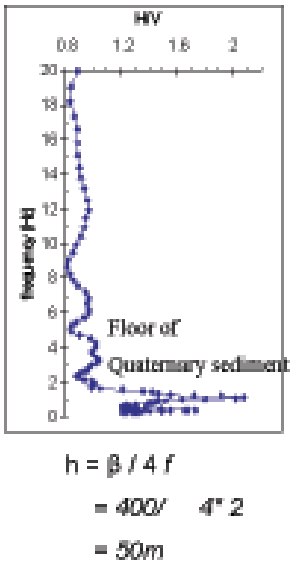

Figure 2.14 Gravel-Silt contacts and its seismic response

Further detailed work using an array of microtremor of seven sets of instruments in circular array is proposed to extract other layers of the basin using Spatial Autocorrelation (SPAC) and Frequency Wave number (f-k) method.

Imtiyaz A Parvez and Dhananjay A Sant

2.10 Ground Motion at Bedrock Level in Delhi City from Himalayan Earthquake Scenarios

The knowledge and characterization of seismic source process and seismic ground motion time histories are two very important items in seismology and earthquake engineering, as they are necessary for seismic hazard assessment. One of the basic tools associated with the study of seismic hazard is the determination of the seismic ground motion time histories at a given site, due to an earthquake of certain magnitude (or moment) at a certain epicentral distance. In order to increase the knowledge in this aspect, a large number of ground motion records are required and in practice however, such a database is not available. In this paper, a preventive tool is proposed, based upon the realistic modeling of ground motion using computer codes developed from the knowledge of the seismic source and of the propagation of seismic waves associated with earthquake scenarios.

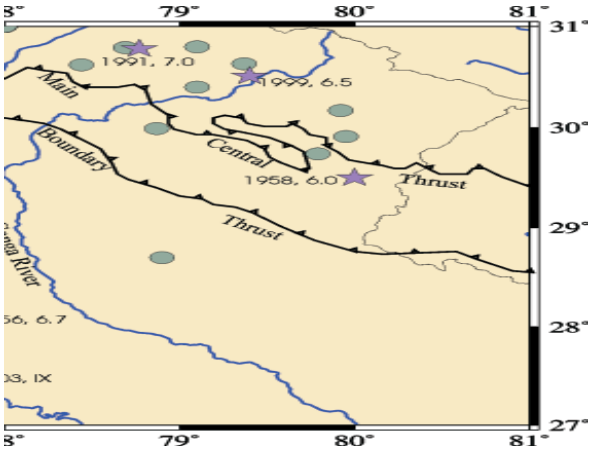

Figure 2.15. The regional map of Delhi and its surrounding areas with the epicenters of the earthquakes, which occurred in the region.

An open question is addressed here: what is the bedrock-level earthquake ground motion in terms of displacement, velocity, acceleration and response spectra in the city to be expected from the sources expected in the so-called seismic gap in the Central Himalayas (Figure 2.15)?

The time histories are simulated using (1) Size Scaled Point Source (SSPS), (2) Extended

Source (ES) and (3) Space and Time Scaled Point Source (STSPS) models. In the first case, the point source (approximation valid when the receiver is at distances greater than the source dimensions) is scaled for its dimensions using a relatively simple spectral scaling law, with zero phase. In the ES case, the seismic waves due to an extended source are obtained by approximating it with a rectangular plane surface, corresponding to the fault plane on which the main rupture process is assumed to occur. The source is represented as a grid of point subsources, and their seismic moment rate functions are generated considering each of them as realizations (sample functions) of a non-stationary random process. Specifying in a realistic way the source length and width, as well as the rupture velocity, one can obtain realistic source time functions, valid in the far-field approximation. In the third case (STSPS), a mixture of extended and point sources has been used. The source time functions generated by the (point) subsources distributed over the fault plane are added in order to obtain the equivalent single source, representative of the entire space and time structure of the extended source, and the related Green function.

The results obtained in this study indicate that the seismic hazard potential in Delhi city due to a possible great earthquake in Central Himalayas is generally high, particularly for long period displacement. The obtained peak displacement are 6.4 cm, 7.8 cm, 8.3 cm for a hypocentral depth 10, 15 and 20 km, respectively, using the SSPS model. The peak velocity is 3.4 cm/s, 3.0 cm/s and 2.3 cm/s for a hypocentral depth 10, 15 and 20 km, respectively, and the peak acceleration is 3.5 cm/s^2, 3.0 cm/s^2 and 3.0 cm/s^2 for the source depth 10, 15 and 20 km for SSPS model. For the STSPS model, the time histories have been compounded considering forward, neutral and reverse rupture as 1720 propagation. The peak amplitudes are obtained always for the reverse rupture propagation. For the source depth of 10 km, the peak displacement is 17.9 cm, the peak velocity is 9. 6 cm/s and the peak acceleration are 5.7 cm/s^2. For the source depth of 15 km, the peak displacement is 21.4 cm, the peak velocity is 8.8 cm/s and the peak acceleration is 4.3 cm/s^2 and for the source depth 20 km the peak displacement is 20.3 cm, peak velocity is 6.7 cm/s and peak acceleration is 2.8 cm/s^2. In the case of ES model, the peak displacement is estimated as 9.1 cm, peak velocity as 3.9 cm/s and peak acceleration as 8.1 cm/s^2 for a source depth of 10 km. For the source depth 15 km, the peak displacement as 11.7 cm, peak velocity as 3.8 cm/s and peak acceleration as 8.3 cm/s^2 has been obtained. For a hypocentral depth of 20 km, peak displacement is estimated as 11.5 cm, peak velocity as 3.0 cm/s and peak acceleration as 6.6 cm/s^2. The example of time histories for vertical component computed for ES model is shown in figures 2.16. Similar figures are obtained for other source model and different components.

The displacement response spectra has been used from the complete time histories in order to characterize the seismic input at Delhi. In fact, not only is it of great significance to the modern displacement-based design engineering approaches, but it is probably the best parameter to characterize the destructiveness potential of earthquakes located at great distances from the target sites, since the energy of the seismic input from these events is mainly concentrated at long periods (e.g. greater than 1 s). It is very important to mention here that the ground motion particularly the displacement at long period has been obtained of the order of ~20 cm which can be converted into MCS intensity in the range of X-XI (Panza et al.,1997). So far,

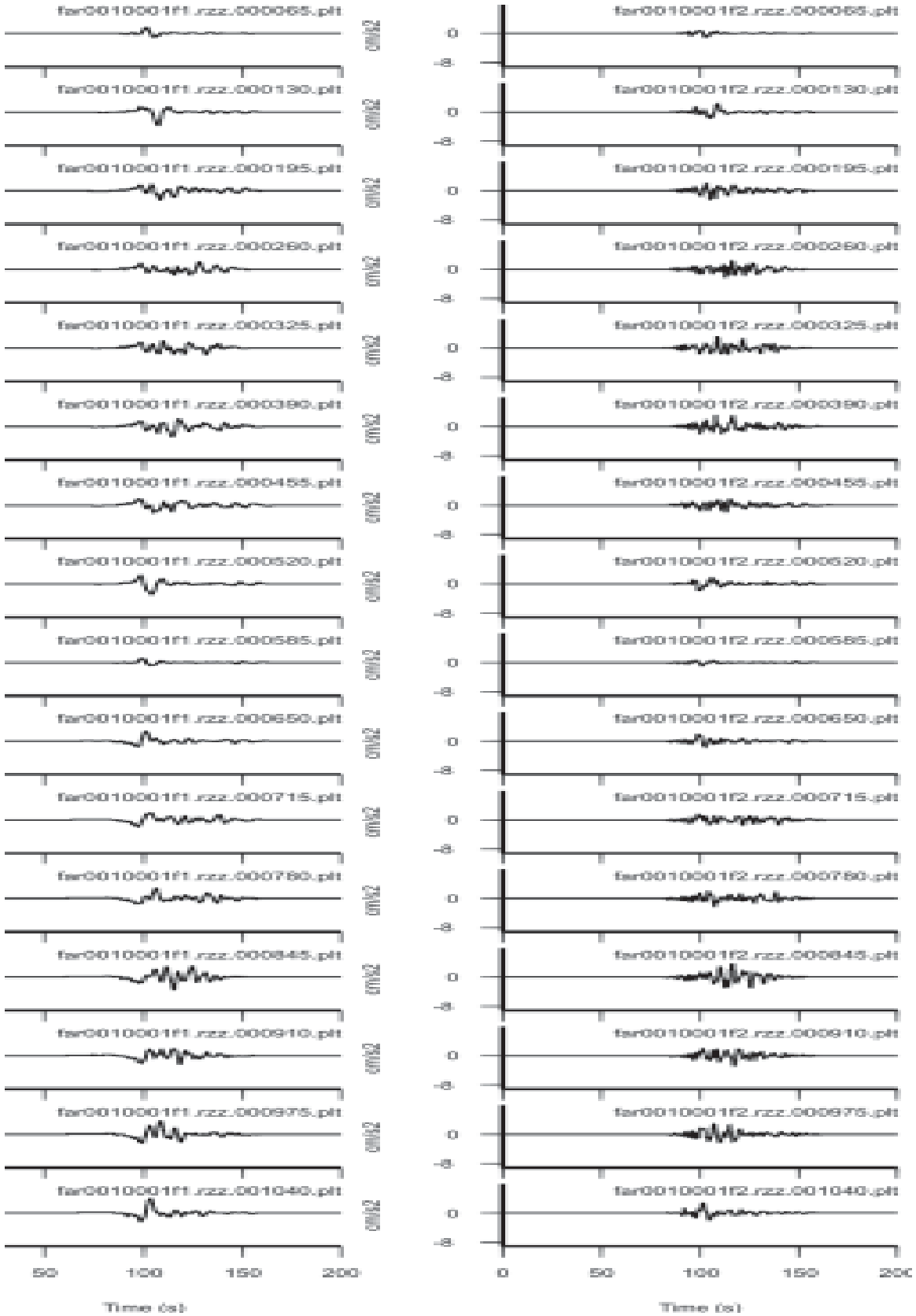

Figure 2.16: Vertical component of synthetic seismograms (displacement (cm), velocity (cm/s), acceleration (cm/s2)) computed at different strike-receiver angles (reported in the left column) computed using ES model and structural model 1 with a central depth of the fault equal to10 km.

such intensities have not been observed in Delhi due to Himalayan earthquake, where as the 1720 earthquake which occurred very close to Delhi had experienced MMI intensity IX (Parvez et al., 2004). Our results can be used as a preventive definition of the seismic hazard in Delhi city without waiting for the great earthquake to occur in Central Himalayas. It can be used reliably to formulate the building codes with a great impact on the effective reduction of their seismic vulnerability.

Imtiyaz A Parvez, Fabio Romanelli and Giuliano F Panza